634–640 Nucleic Acids Research, 1995, Vol. 23, No. 4

In vivo analyses of the internal control region in the 5S rRNA gene from *Saccharomyces cerevisiae*

Yoon Lee, Alexander M. Erkine, Don I. Van Ryk and Ross N. Nazar*

Department of Molecular Biology and Genetics, University of Guelph, Guelph, Ontario N1G 2W1, Canada

Received October 17, 1994; Revised and Accepted January 3, 1995

ABSTRACT

The internal control region of the *Saccharomyces cerevisiae* 5S rRNA gene has been characterized *in vivo* by genomic DNase I footprinting and by mutational analyses using base substitutions, deletions or insertions. A high copy shuttle vector was used to efficiently express mutant 5S rRNA genes *in vivo* and isotope labelling kinetics were used to distinguish impeded gene expression from nascent RNA degradation. In contrast to mutational studies in reconstituted systems, the analyses describe promoter elements which closely resemble the three distinct sequence elements that have been observed in *Xenopus laevis* 5S rRNA. The results indicate a more highly conserved structure than previously reported with reconstituted systems and suggest that the saturated conditions which are used in reconstitution studies mask sequence dependence which may be physiologically significant. Footprint analyses support the extended region of protein interaction which has recently been observed in some reconstituted systems, but mutational analyses indicate that these interactions are not sequence specific. Periodicity in the footprint provides further detail regarding the *in vivo* topology of the interacting protein.

INTRODUCTION

Since first observed in the *Xenopus* 5S rRNA gene (1,2), the internal control region for RNA polymerase III transcribed genes has been widely characterized both with respect to gene type and divergent origins (3). While the initial studies on the *Xenopus* 5S rRNA gene give rise to a basic model for the class III gene internal control region (ICR), recent studies have indicated a surprising divergence in the arrangement of the promoter elements. In *Neurospora crassa*, for example, an upstream element at nucleotides –24 to –29 and internal elements at +19 to +30, +44 to +57 and +73 to +103 are essential for 5S rRNA gene transcription, but in *Drosophila melanogaster* a larger upstream element from nucleotide –26 to –39 and four intragenic elements located at +3 to +18, +37 to +44, +48 to +61 and +78 to +98 have been documented (4–6).

In view of the ease with which yeast cells can be manipulated, genetically and biochemically, *Saccharomyces cerevisiae* has emerged as a major organism for studies on the RNA polymerase III transcription system, especially *in vitro* reconstitutions using purified components. The three major transcription factors, TFIIIA (7) TFIIIB (8–10) and TFIIIC (11–15), have been largely or fully purified to homogeneity and extensive studies on reconstituted transcription complexes have been undertaken based on both mutational and footprinting analyses. Despite the systematic nature of these studies, striking differences in the conclusions appear to remain. Using deletion–substitution mutations, Challice and Segall (16), for example, concluded that two promoter elements were essential, one spanning the start site from nucleotide –14 to +8 and a short internal control region from +81 to +94. In contrast, using DNase I footprinting, Geiduschek and co-workers (13,17–19) concluded that with a complete transcription system, protein interactions extend over the entire transcription unit, together with almost 50 bp of 5′ flanking sequence.

To further clarify these contrasting observations, we are using both mutational and footprint analyses to examine yeast 5S rRNA gene expression *in vivo*. In previous studies on the structure and assembly of the 5S rRNA we were able to efficiently express mutant 5S rRNA genes *in vivo*, giving rise to ribosome populations which were ~80–90% mutant (20,21). In the present study, this approach has been used extensively, together with DNase I genomic footprinting, to define the essential sequence elements and regions of protein interaction under normal growth conditions.

MATERIALS AND METHODS

Construction and expression of mutant 5S rRNA genes

Mutations were introduced into a yeast 5S rRNA gene (22) containing a structural marker mutation (23,24) either by the methods of Kunkel (25) or by a modified two-step PCR procedure (26). Mutant oligonucleotides and PCR primers were synthesized using a Cyclone Plus automated DNA synthesizer (Millipore Corp., Milford, MA) and each mutation was confirmed by DNA sequencing (27). Mutant genes were cloned into pYF404, a high copy (30–40 copies/cell) yeast shuttle vector (28); the recombinant plasmids were purified and used to transform a *LEU2*-deficient yeast strain (AH22) as described by Hinnen *et al.* (29).

Analysis of mutant 5S rRNA expression

For all analyses, transformed cells were grown with shaking under selective conditions at 30°C and whole cell RNA was

* To whom correspondence should be addressed

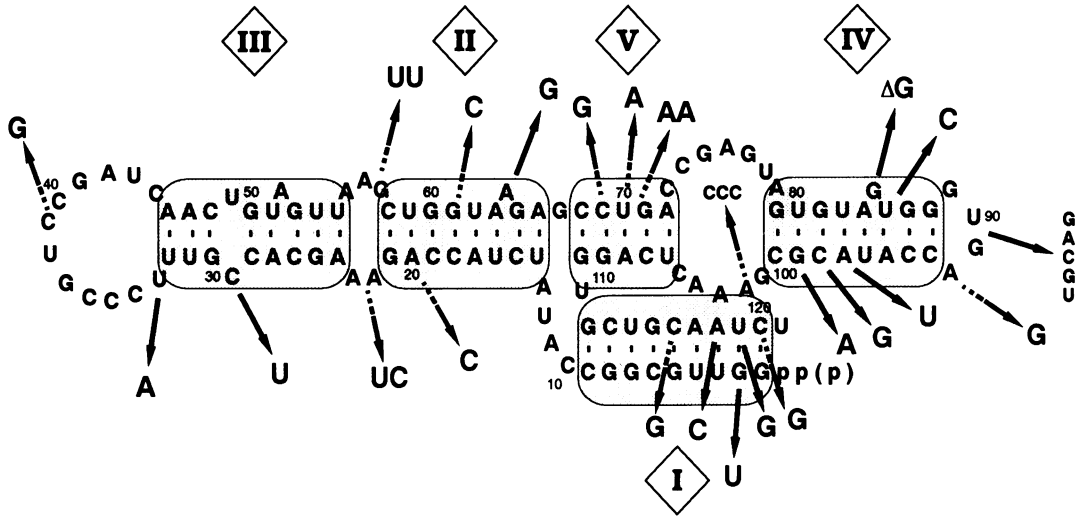

Figure 1. Effect of mutations on the stability of 5S rRNA from *S.cerevisiae*. Mutations were introduced by primer extension or PCR amplification and mutant genes were expressed *in vivo* as described in Materials and Methods. The stability of the resultant RNAs was assessed by labelling kinetics; stable RNAs are differentiated from significantly unstable molecules by the solid and broken arrows respectively. The consensus secondary structure is that of Nishikawa and Takemura (41). Conserved helical regions are shaded and identified by the numerals (I–V) above or below.

prepared by sodium dodecyl sulphate–phenol extraction as previously described (23). The 5S rRNA fraction was purified on an 8% polyacrylamide gel containing 8 M urea, redissolved in 7 M urea and further analysed on 12% non-denaturing or denaturing polyacrylamide gels at room or elevated temperatures, as appropriate. Autoradiography or methylene blue stain (30) were used to detect the different RNA constituents; for quantitative analyses the fractionated bands were scanned using a Model 620 CCD densitometer (Bio-Rad, Richmond, CA) or counted using a scintillation counter.

When 5S rRNA expression and stability were evaluated by RNA labelling kinetics, cells were grown in selective minimal medium to an absorbancy of 0.4–0.6 at 550 nm, harvested by centrifugation, washed twice with distilled water and resuspended in low phosphate medium (31). After 1–2 h of further growth at 30°C, the cells were labelled briefly for 2–15 min with 50–500 μCi of [^{32}P]orthophosphate and collected by filtration on glass microfibre filters. The RNA was extracted with SDS–phenol at 65°C (32), fractionated on polyacrylamide gels and the autoradiographs were scanned to quantify the 5S rRNA bands as described above. For pulse-chase analyses, the briefly labelled culture was diluted with an equal volume of normal phosphate-buffered medium and aliquots were again collected by filtration at appropriate times.

The plasmid copy number was determined by hybridization analyses as previously described (20) using a nick-translated yeast *LEU2* gene as a probe. Autoradiographs were scanned as described above and the plasmid copy number was calculated from the intensity of the plasmid band and the alternately migrating genomic *LEU2* band.

Genomic footprint analysis

Genomic footprints were determined by methods based on those described by Huibregtse and Engelke (33) and modifications by Diffley and Cocker (34). Mid log phase cultures (100 ml) of *S.cerevisiae* (strain AH22) were grown with aeration at 30°C in selective (0.67% yeast nitrogen base without amino acids, 2% dextrose, 20 μg/ml histidine) or non-selective (1% yeast extract, 2% peptone, 2% dextrose) medium, harvested, washed and resuspended in 3 ml of 1 M sorbitol, 1 mM EDTA, 3 mM dithiothreitol containing 2 mg/ml (~3000 μ) lyticase (Sigma Chemical Co., St Louis, MO). The resulting spheroplasts were lysed in buffer containing 10 mM Tris–HCl, pH 7.5, 10 mM $MgCl_2$, 5 mM 2-mercaptoethanol, 1 mM phenylmethylsulphonyl fluoride, 2 μg/ml leupeptin and 1 μg/ml pepstatin and 300 μl aliquots were treated with 1–16 μl of DNase I (5 mg/ml) for 5 min at room temperature. Following the addition of an equal volume of 50 mM Tris–HCl, pH 7.5, containing 1 M NaCl, 1% sodium dodecylsulfate, 50 mM EDTA, the DNA was extracted twice with phenol/chloroform (1:1), precipitated with 2-propanol, treated with Rnase A and extracted further with phenol/chloroform. After precipitation with ethanol, the DNA was dissolved in water (2 μg/μl). For control DNA digestions, genomic DNA was prepared as described above without DNase I treatment.

The cleavage sites were detected by repeated primer extension with *Taq* polymerase using 20 cycles of 1 min at 94°C, 1 min at 42°C and 2 min at 72°C and 10 μg of template DNA. For chromosomal analyses, the oligonucleotide primer (5′-TAAAT-ATTGTCCTCCAC-3′) was labelled using polynucleotide kinase and [γ-^{32}P]ATP (7000 Ci/mmol) and primer of equal specific activity was prepared by polyacrylamide gel electrophoresis (35). Standard dideoxy sequencing reactions using *Taq* polymerase and the same primer and thermal cycle were carried out as chain length markers. For transformed cell analyses, a plasmid-specific primer (5′-CCACGATGCGTCCGGCGTAG-3′) was used for the sequence analyses.

RESULTS AND DISCUSSION

In earlier studies on the structure and function of the 5S rRNA (20,21), mutations were systematically introduced into all regions of the yeast 5S rRNA gene (see Fig. 1 for a summary) and the mutated genes were expressed *in vivo* to detect those which

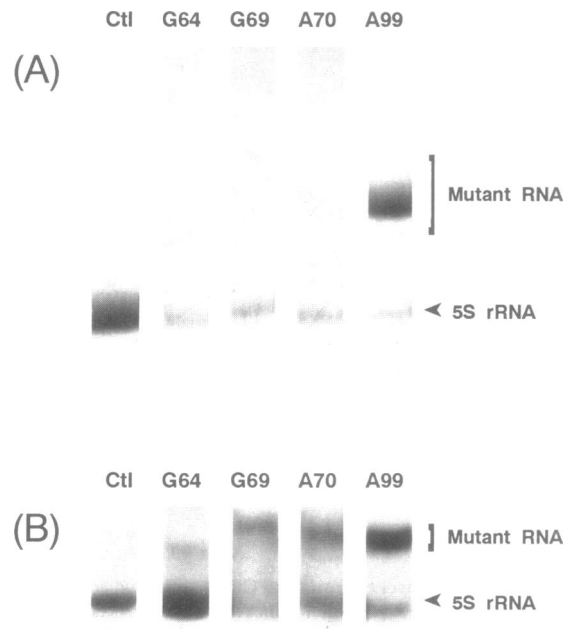

Figure 2. Detection of unstable 5S rRNA mutations in *S.cerevisiae*. Normal or mutant RNA was prepared from unlabelled (**A**) or ^{32}P-labelled (**B**) cells and fractionated on 12% non-denaturing polyacrylamide gels as previously described (23). The 5S rRNAs were detected with methylene blue stain or autoradiography. The positions of normal 5S rRNA are indicated by arrows and the mutant nucleotide is identified above each lane.

adversely affected the growth rate or ribosome assembly. The resultant yeast transformants could be grouped into three categories. Several of the mutant genes significantly reduced the growth rate and, presumably, a few appeared to be lethal, as no transformants could be recovered. Most, however, had no effect on the growth rate, either because the changes in the 5S rRNA could be accommodated in the ribosome structure or little mutant RNA was present. When accommodated in the ribosome structure, our previous analyses of the cellular RNA content indicated that expression of the 5S rRNA was strictly regulated and even when 80% of the 5S rRNA population was mutant, the total 5S rRNA content remained constant when compared with the 5.8S rRNA (20,23). These results strongly suggest that, although the plasmid-associated genes are preferentially expressed, they are still subject to strict regulation with respect to the cellular 5S rRNA content. In this study, the last group of mutations which resulted in little or no mutant RNA was characterized further to determine nucleotides which were essential for efficient 5S rRNA gene expression *in vivo*.

Because low levels of mutant RNA could reflect either impeded gene expression or an unstable and rapidly degraded RNA structure, the stability of each mutant RNA was determined using isotope labelling kinetics. Mutant RNAs were again detected by their differential electrophoretic mobilities on non-denaturing gels. To avoid or minimize complex fractionations due to multiple conformations, the RNA was dissolved and loaded on gels in 7 M urea. Under the conditions which were used, all mutant RNAs were observed to migrate as discrete bands and gels did not reveal significant amounts of minor conformations or heterogeneous streaks (e.g. Fig. 2A); the positions of normal and mutant 5S rRNA bands were confirmed by RNA sequencing as previously described (20). As also illustrated by the examples shown in Figure 2, when compared with a previously characterized and stable marker mutation (Y5A99) a number of mutations resulted in very low steady-state levels of mutant RNA relative to RNA encoded by the host cell genes. In the three examples shown (G64, G69, A70), the intensity of the mutant RNA band is only a fraction of the normal RNA, while the amount of Y5A99 (A99) is clearly many times greater. The reason for this differed depending on each mutation. As shown in the lower panel (B), brief labelling could result in very different levels of mutant RNA. Relative to host gene encoded 5S rRNA, at 2 min very little Y5G64 is labelled, but much larger amounts of Y5G69 are present and intermediate amounts of Y5A70 are present. These results indicate that Y5G69 is efficiently expressed but rapidly degraded, whereas Y5G64 appears to be stable but poorly expressed. Again, Y5A70 is intermediate in that its expression is partially inhibited and the resulting 5S rRNA molecule is moderately unstable. Previous analyses of unstable examples have suggested that at least some of the unstable mutant RNAs are incorporated into subunits and even polyribosomes, but subsequently lead to 60S subunit degradation and subunit imbalances (20). In contrast to all three examples, levels of marker mutant RNA (Y5A99) were observed to be high in both cases. A quantitative summary for all the mutants which were characterized is presented in Table 1, together with the plasmid copy number. While some variation in the copy number was observed, all were similar to that observed with cells transformed with plasmid containing only a wild-type 5S rRNA gene (pYF5), eliminating the possibility that different levels of RNA reflected a variable copy number.

To further ensure that rapid degradation of unstable mutant RNAs did not erroneously indicate an inhibited gene expression, degradation kinetics of mutants in putative regulatory sequences were examined and the half-life was determined for each mutant RNA. As indicated in Table 2, with unstable RNAs the half-life was 0.8–2.1 h, while for the normal 5S rRNA and the remaining examples the half-life was about 1–1.5 days. An accurate measurement of these longer half-lives was somewhat more difficult, as the cultures matured before a significant degradation occurred. Nevertheless, the substantially longer half-lives confirmed the lack of significant RNA degradation and a clear inhibition of gene expression. With all examples in Table 2, the initial level of mutant 5S rRNA was also determined, to include corrections for the half-life and the plasmid copy number. As indicated, the effect of these corrections was very small in every instance.

When compared with the generalized model shown in Figure 1, the stability of mutant RNA molecules was clearly not directly predictable from the consensus secondary structure, an observation which underlines the complex tertiary structure that has been reported for at least the eukaryotic 5S rRNA (21). For example, mutants such as Y5G69 or Y5A70, which disrupt a conserved helix (V), did result in unstable molecules, but with other mutants such as Y5U97 or Y5G98 which also disrupt a conserved helix (IV) the mutant RNA population remained high, indicating that these molecules did not degrade rapidly. Furthermore, the effects of changes in bulges or loops also differ greatly. For example, Y5A33 is stable, but Y5G92 is unstable. Both of these loop regions were previously shown to be incorporated in the tertiary structure (21,36) and the mutant RNA molecules are being chemically probed to determine the structural nature of the instability.

Table 1. Expression and stability of mutant 5S rRNA

Mutation	Plasmid copy number[a]	Mutant RNA Briefly labelled[b]	Steady-state[c]
pYF5	32.2	NA[d]	NA
pYF5-A1	31.5	79.1	80.1 ± 3.7
pYF5U2	26.0	71.0	78.6 ± 2.5
pYF5C20	28.7	76.8	20.7 ± 2.2
pYF5C22U23	27.0	84.1	ND[e]
pYF5U29	34.5	83.4	81.7 ± 5.1
pYF5A33	38.1	72.4	83.0 ± 2.4
pYF5G39	39.6	83.7	64.9 ± 2.1
pYF5U56U57	25.5	48.9	9.3 ± 1.9
pYF5C61	33.3	28.3	10.4 ± 2.4
pYF5G64	34.9	15.3	14.9 ± 2.9
pYF5G69	28.6	78.4	9.1 ± 2.1
pYF5A70	26.6	39.7	10.9 ± 1.6
pYF5A70A71	34.5	21.2	ND[e]
pYF5ΔG85	26.4	17.5	17.6 ± 3.2
pYF5C86	36.8	17.2	16.2 ± 2.6
pYF5iU90-5	26.5	17.5	18.2 ± 3.4
pYF5G92	29.9	86.2	33.3 ± 1.7
pYF5U97	33.4	76.5	82.5 ± 2.1
pYF5G98	36.4	70.7	65.6 ± 5.7
pYF5A99	32.7	79.8	78.2 ± 2.7
pYF5C101C102C103	34.4	84.3	5.5 ± 1.9
pYF5G116	31.9	73.2	5.8 ± 4.1
pYF5C118	31.6	77.1	63.3 ± 2.3
pYF5G119	24.5	69.4	60.6 ± 3.9
pYF5G120	40.8	80.6	41.1 ± 1.2

[a]Ratio between the plasmid and genome-associated *LEU2* gene as determined by hybridization analysis.
[b]Per cent radioactive mutant RNA after 2 min of labelling and acrylamide gel fractionation.
[c]Per cent mutant RNA after acrylamide gel fractionation and quantification after methylene blue staining. Values are the average of 2–4 determinations ± SE.
[d]NA, not applicable.
[e]ND, none detected.

When the RNA expression levels which are summarized in Table 1 were examined with respect to previous analyses of internal promoter elements, the results were not consistent with *in vitro* studies of yeast 5S rRNA expression, but more strongly reflected earlier analyses in *Xenopus*. As shown in Figure 3, mutations which substantially reduced the transcription of 5S rRNA were observed in regions that corresponded with all three consensus promoter sequence elements in *Xenopus* and even extensions as detected by site-directed mutagenesis (37). Although the short spacers between the extensions were not examined, in contrast to studies on the transcription of deletion–substitution mutations *in vitro* (16), both box A and M sequence elements clearly have very substantial effects on 5S rRNA expression and changes at the 5′ end of the coding sequence appear not to influence gene expression. Furthermore, mutations in the additional sequence elements which appear to interact with protein in reconstituted transcription complexes (17,18) also did not significantly influence transcription of the yeast 5S rRNA *in vivo*. As indicated in Figure 3, none of the mutations in regions which have been demonstrated *in vitro* to be protected by TFIIIC or RNA polymerase showed a significant influence on transcription.

Table 2. Half-life of mutant 5S rRNA

Mutation	Half-life[a]	Initial concentration[b]
5S rRNA	37.3	100.0
pYF5U56U57	1.5	52.5
pYF5C61	2.1	27.6
pYF5G64	18.2	14.1
pYF5A70	1.4	44.5
pYF5A70A71	0.8	18.8
pYF5ΔG85	28.1	20.2
pYF5C86	28.8	13.1
pYF5iU90i5	38.5	20.6
pYF5A99	35.1	74.5

[a]Transformed cell cultures were briefly labelled in low phosphate medium, diluted with normal phosphate-buffered medium and the half-life in hours was determined from the radioactivity of the mutant RNA as determined from aliquots sampled over a 12 h period.
[b]Initial per cent mutant RNA as determined from the briefly labelled (2 min) sample (Table 1), but corrected for instability using the half-life and normalized for an average plasmid copy number of 30.

To further examine these differences, the yeast 5S rRNA gene was also examined by DNase I genomic footprinting. Yeast cells or purified yeast genomic DNA were treated with a wide range of nuclease concentrations to determine effective and equivalent levels of digestion and cleaved fragments were detected by PCR-amplified DNA sequencing (33). As shown in Figure 4, under appropriate digestion conditions, differences due to protein protection could be readily detected in many regions of the 5S rRNA sequence. Although the patterns were less pronounced than observed *in vitro* under saturated conditions, reproducible profiles were observed which likely reflect an average for genes in diverse functional states. Both host cell genomic 5S rRNA genes and plasmid-associated genes were examined using genome or plasmid-specific primers with comparable results, strongly suggesting that the genes were equivalent with respect to the assembled initiation complex. Such results indicate that the preferential expression of the plasmid-associated genes is likely the result of additional factors; for example, the local concentration of nucleotides, RNA polymerase, etc., which may be significantly lower in regions of the genome where 5S rRNA genes are closely and tandemly arranged with genes encoding the other ribosomal RNAs.

As is clearly evident with the naked DNA (Fig. 4), sequence bias in DNase I digestion results in substantial differences in the degree of cleavage and subsequent band intensity between the different nucleotides. To eliminate this bias in the interpretation

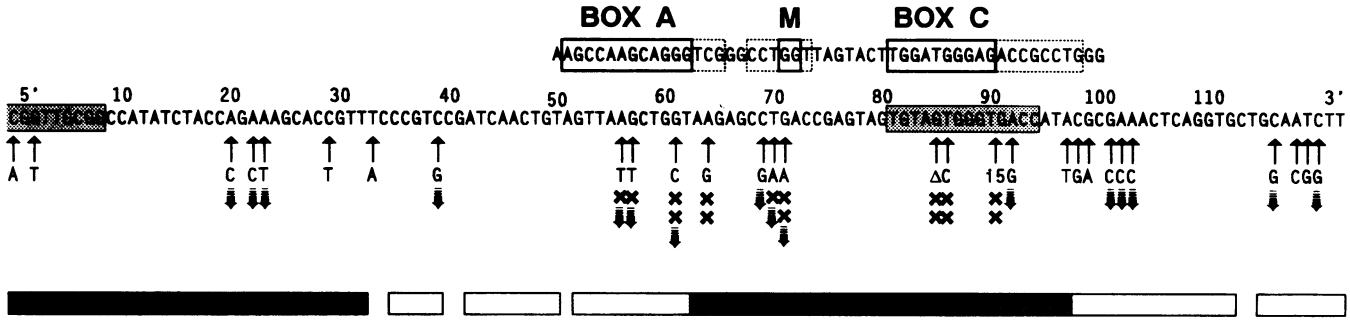

Figure 3. Effect of mutations on the expression of the 5S rRNA gene in *S.cerevisiae*. Mutant 5S rRNA genes were expressed as described in Figure 1 and unstable 5S rRNA products were detected as described in Figure 2. Moderately or largely inhibited genes are indicated by one or two Xs and significantly unstable RNA products are identified by the broken arrows. The box A element, intermediate element (M) and box C element are those previously identified in *Xenopus* (37) and the shaded sequences are promoter elements previously identified in *Saccharomyces* (16). The light, intermediate and darkly shaded boxes are specific binding sites for TFIIIC, TFIIIA and PolIII, as defined by Kassavetis and co-workers (18).

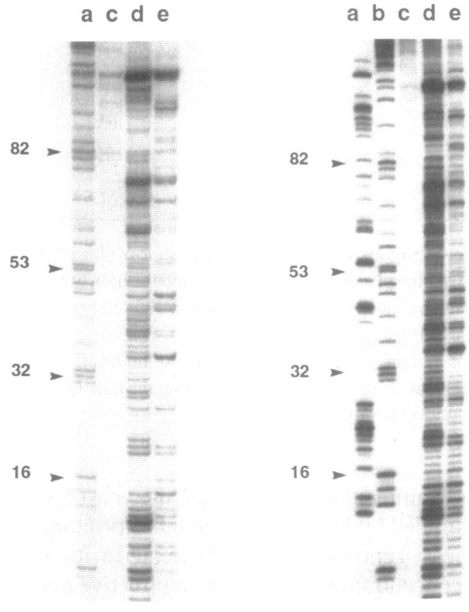

Figure 4. Footprint analyses for the coding strand of host cell or plasmid-associated 5S rRNA genes in *S.cerevisiae*. Spheroplast lysates were prepared from normal (left) or plasmid-transformed (right) cells, treated with DNase I and DNA was purified as described in Materials and Methods. A 5′ end-labelled oligonucleotide complementary to the coding strand was annealed with 20 µg DNase I-treated genomic (lane e) or naked (lane d) DNA and primer (host cell or plasmid-specific primer) extended with *Taq* polymerase in 20 cycles of 1 min at 94°C, 1 min at 42°C and 2 min at 72°C. Undigested DNA (lane c) is included as a control and standard A or T sequencing reactions (lanes a or b) using the same oligonucleotide and *Taq* polymerase are included as chain length markers. The numbered arrows identify residues corresponding to the 5S rRNA.

of the genomic analyses, the gels were scanned and the data were normalized at each residue with the degree of cleavage being determined as a percentage of that observed with naked DNA. The 100% value was taken as the average of all of the highest values (±10%) across the entire gene and surrounding spacers. Again, similar results were obtained with both genomic and plasmid-associated genes (the results of three replicate experiments for the plasmid-associated gene are summarized in the histogram shown in Figure 5). Most residues were readily quantified; those at the 3′ end which were very weak and poorly resolved were omitted. As anticipated, a substantial protection was observed in the sequences which corresponded to known ICR elements (i.e. boxes A, C and M), including the extended regions. In general, however, protection was observed over most of the 5S rRNA sequences, as previously noted with the reconstituted yeast 5S rRNA transcription system (18). This extended region of protection has also been observed in studies on the *Xenopus* gene system (38,39).

An additional feature which is evident in the present footprint analysis is a periodicity in the extended region of protein protection. As noted in Figure 5, the protection in the 5′-half of the internal sequence is essentially cyclical, with five equivalent regions (a–e) based on a 10 nt repeat. Again, this more closely resembles earlier footprinting with the *Xenopus* gene for 5S rRNA (40). Although less certain, a similar periodicity seems to be present at the 3′ end. As a 10 bp periodicity corresponds with a turn of the DNA helix, the data strongly suggest that the protein basically interacts with one side of the DNA helix or that the DNA is wound on the protein. Indeed, a similar observation by other workers (34) in studies on the yeast replication origin has been taken as evidence of a nucleosome structure. Whatever the case, this is strikingly different from the internal control region (nt 50–100), which is more uniformly protected except for consistent hypersensitivity at residues 87 and 88. Although the overall intensity of cleavage at this site was always relatively low (e.g. Fig. 4), in each of four experiments the normalized data always revealed a more sensitive site of enzyme digestion in the genomic DNA complex. In some experiments, hypersensitivity was also observed at A66 and G67 (see Fig. 4), but this was not reproducible and cleavage at these positions in the untreated lane suggest they may result from non-specific cleavage during sample preparation.

To further confirm the significance of sequence specificity outside the C element sequence, one of the mutants which resulted in a substantial inhibition of 5S rRNA expression (pYF5A70A71) was also examined by DNase I genomic footprinting. In this case, a plasmid sequence-specific primer was again used to exclude signals from the chromosomal DNA. As shown in Figure 6, the analyses demonstrated significant changes in the extended protection over the ICR elements (i.e. boxes A, C and M). Instead, the 10 bp periodicity (a–e) appears to be

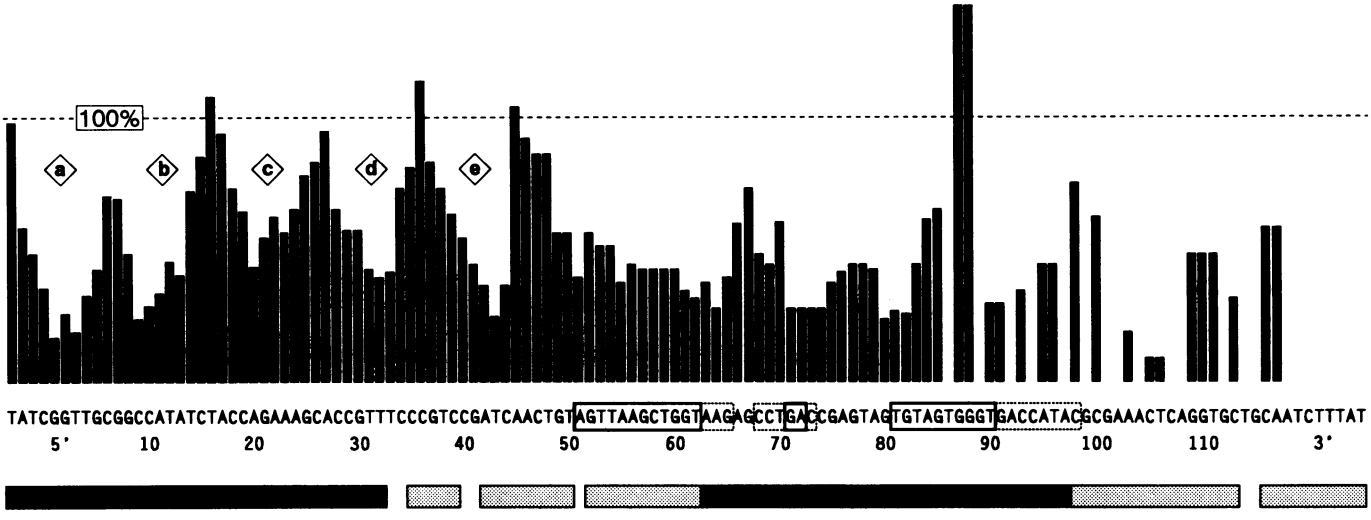

Figure 5. Comparison of the DNase I digestion footprint in genomic and naked 5S rDNA from *S.cerevisiae*. Autoradiographs of the footprint analyses as described in Figure 4 were scanned and the extent of digestion at each residue in the chromatin is shown in the histogram as a percentage of the digestion observed with naked DNA. Residue numbers correspond to the 5S rRNA and periodicity in the digestion profile is identified as a–e. Enclosed residues correspond to identified internal control elements and shaded boxes correspond to identified binding sites for individual components in transcription complexes as described in Figure 3.

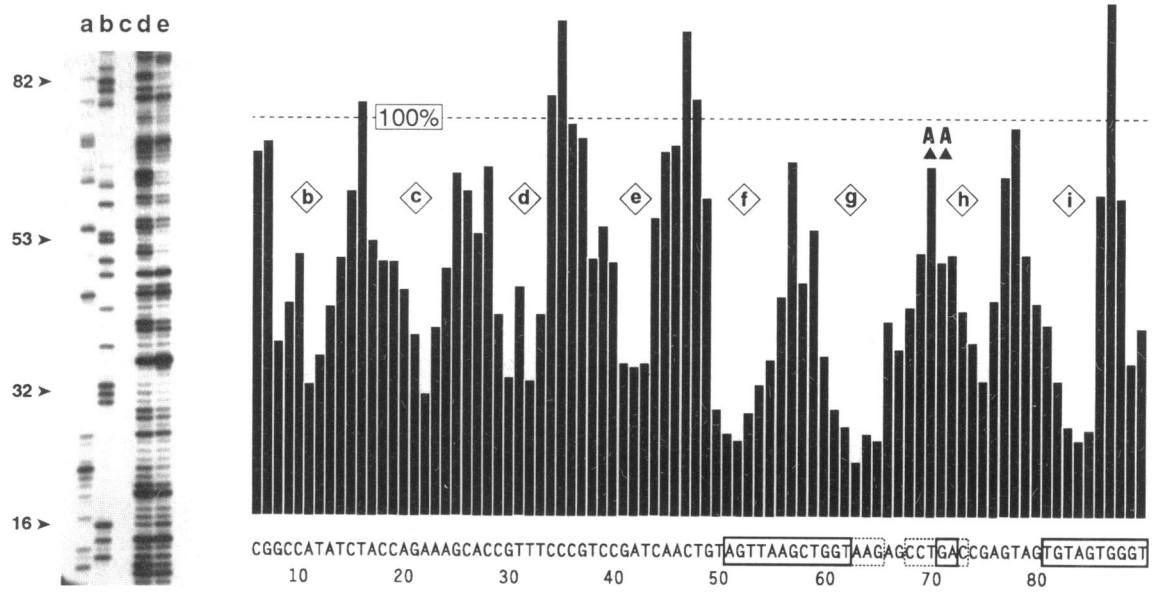

Figure 6. Comparison of the DNase I digestion footprint in genomic and naked mutant 5S rDNA from *S.cerevisiae*. DNA was prepared from cells transformed with pYF5A70A71, treated with DNase I as described in Figure 4 and primer extended with *Taq* polymerase using a plasmid sequence-specific primer before fractionation by polyacrylamide gel electrophoresis (left). Treated genomic (lane e) and naked (lane d) DNA samples were applied together with an undigested control (lane c) as well as normal A- (lane a) and T-specific (lane b) sequencing reaction products as chain length markers. The autoradiographs of the footprint analyses were scanned and the extent of digestion at each residue is shown in the histogram (right) as a percentage of the digestion observed with naked DNA. Residues in the 5S rRNA and internal control elements are identified below to correspond with Figure 5. The extended periodicity in the digestion profile is identified as b–i.

extended over this region (f–i). Again, the nature of the interacting proteins can only be suggested from earlier reconstitution analyses, but the importance of the nucleotide sequence is obvious.

In summary, therefore, the present study provides new *in vivo* evidence for a conserved internal control region in *S.cerevisiae* consistent with the three sequence elements which have been reported in other organisms. Genomic footprint analyses support the extended interaction with protein revealed in reconstitution studies, but indicate that the additional protein is localized on one side of the DNA helix and the mutations suggest that these extended interactions are partially or entirely independent of the nucleotide sequence. It continues to be reasonable to speculate that the extra contacts may be oriented by the internal control region, but a normal nucleosome structure also provides a simple explanation and raises the possibility that the *in vitro* studies

reflect a system saturated with transcriptional apparatus, while the present genomic footprint better reflects the normal state of the 5S rRNA gene *in vivo*. This saturation may also explain the insensitivity of reconstitution studies to ICR elements A and M, underlining the importance of parallel analyses *in vivo*. Mutational and footprint analyses continue on the upstream regions to further define any functional significance in the extended regions of protein interaction.

ACKNOWLEDGEMENT

This study was supported by the Natural Sciences and Engineering Research Council of Canada.

REFERENCES

1 Bogenhagen, D.F., Sakonju, S. and Brown, D.D. (1980) *Cell*, **19**, 27–35.
2 Sakonju, S., Bogenhagen, D.F. and Brown, D.D. (1980) *Cell*, **19**, 13–25.
3 Geiduschek, E.P. and Tocchini-Valentini, G.P. (1988) *Annu. Rev. Biochem.*, **57**, 873–914.
4 Shi, Y. and Tyler, B.M. (1991) *J. Biol. Chem.*, **266**, 8015–8019.
5 Garcia, A.D., O'Connell, A.M. and Sharp, S.J. (1987) *Mol. Cell. Biol.*, **7**, 2046–2051.
6 Sharp, S.J. and Garcia, A.D. (1988) *Mol. Cell. Biol.*, **8**, 1266–1274.
7 Wang, C.K. and Weil, P.A. (1989) *J. Biol. Chem.*, **264**, 1092–1099.
8 Klekamp, M.S. and Weil, P.A. (1986) *J. Biol. Chem.*, **261**, 2819–2827.
9 Kassavetis, G.A., Bartholomew, B., Blanco, J.A., Johnson, T.E. and Geiduschek, E.P. (1991) *Proc. Natl. Acad. Sci. USA*, **88**, 7308–7312.
10 Kassavetis, G.A., Joageiro, C.A.P., Piaano, M., Geiduschek, E.P., Colbert, T., Hahn, S. and Blance, J.A. (1992) *Cell*, **71**, 1055–1064.
11 Gabrielsen, O.S., Marzouki, N., Ruet, A., Sentenac, A. and Fromageot, P. (1989) *J. Biol. Chem.*, **264**, 7505–7511.
12 Johnson, D.L. and Wilson, S.L. (1989) *Mol. Cell. Biol.*, **9**, 2018–2024.
13 Kassavetis, G.A., Riggs, D.L., Negri, R., Nguyen, L.H. and Geiduschek, E.P. (1989) *Mol. Cell. Biol.*, **9**, 2551–2566.
14 Parsons, M.C. and Weil, P.A. (1990) *J. Biol. Chem.*, **265**, 5095–5103.
15 Bartholomew, B., Kassavetis, G.A., Braun, B.R. and Geiduschek, E.P. (1990) *EMBO J.*, **9**, 2197–2205.
16 Challice, J.M. and Segall, J. (1989) *J. Biol. Chem.*, **264**, 20060–20067.
17 Braun, B.R., Riggs, D.L., Kassavetis, G.A. and Geiduschek, E.P. (1989) *Proc. Natl. Acad. Sci. USA*, **86**, 2530–2534.
18 Kassavetis, G.A., Braun, B.R., Nguyen, L.H. and Geiduschek, E.P. (1990) *Cell*, **60**, 235–245.
19 Braun, B.R., Bartholomew, B., Kassavetis, G.A. and Geiduschek, E.P. (1992) *J. Mol. Biol.*, **228**, 1063–1077.
20 Van Ryk, D.I., Lee, Y. and Nazar, R.N. (1992) *J. Biol. Chem.*, **267**, 16177–16181.
21 Van Ryk, D.I. and Nazar, R.N. (1992) *J. Mol. Biol.*, **226**, 1027–1035.
22 Szostak, J.W. and Wu, R. (1979) *Plasmid*, **2**, 536–554.
23 Van Ryk, D.I., Lee, Y. and Nazar, R.N. (1990) *J. Biol. Chem.*, **265**, 8377–8381.
24 Nazar, R.N., Van~Ryk, D.I., Lee, Y. and Guyer, C.D. (1991) *Biochem. Cell Biol.*, **69**, 217–222.
25 Kunkel, T.A. (1985) *Proc. Natl. Acad. Sci. USA*, **82**, 488–492.
26 Good, L. and Nazar, R.N. (1992) *Nucleic Acids Res.*, **20**, 4934.
27 Sanger, F., Nicklen, S. and Coulson, A.R. (1977) *Proc. Natl. Acad. Sci. USA*, **74**, 5463–5467.
28 Percival-Smith, A. and Segall, J. (1987) *Mol. Cell. Biol.*, **7**, 2484–2490.
29 Hinnen, A., Hicks, J.B. and Fink, G.R. (1978) *Proc. Natl. Acad. Sci. USA*, **75**, 1929–1933.
30 Peacock, A.C. and Dingman, C.W. (1967) *Biochemistry*, **6**, 1818–1827.
31 Rubin, G.M. (1973) *J. Biol. Chem.*, **248**, 3860–3875.
32 Steele, W.J., Okamura, N. and Busch, H. (1965) *J. Biol. Chem.*, **240**, 1742–1749.
33 Huibregtse, J.M. and Engelke, D.R. (1991) *Methods Enzymol.*, **194**, 550–562.
34 Diffley, J.F.X. and Cocker, J.H. (1992) *Nature*, **357**, 169–172.
35 Maxam, A.M. and Gilbert, W. (1980) *Methods Enzymol.*, **65**, 499–560.
36 Nazar, R.N. (1991) *J. Biol. Chem.*, **266**, 4562–4567.
37 Pieler, T., Ham, J. and Roeder, R.G. (1987) *Cell*, **48**, 91–100.
38 Wolffe, A.P. and Morse, R.H. (1990) *J. Biol. Chem.*, **265**, 4592–4599.
39 Chipev, C.C., and Wolffe, A.P. (1992) *Mol. Cell. Biol.*, **12**, 45–55.
40 Rhodes, D. (1985) *EMBO J.*, **4**, 3473–3482.
41 Nishikawa, K. and Takemura, S. (1974) *FEBS Lett.*, **40**, 106–109.